MATCH
Communications in Mathematical and in Computer Chemistry

MATCH Commun. Math. Comput. Chem. **64** (2010) 373-390

ISSN 0340 - 6253

HOMO–LUMO Maps for Chemical Graphs

Patrick W. Fowler
Department of Chemistry, University of Sheffield, Sheffield S3 7HF, UK
P.W.Fowler@sheffield.ac.uk

Tomaž Pisanski
Department of Theoretical Computer Science, IMFM, University of Ljubljana, Jadranska 19, 1000 Ljubljana, Slovenia
tomaz.pisanski@fmf.uni-lj.si

(Received February 1, 2010)

Abstract

Electron configurations of π systems are represented on the HOMO-LUMO map: a scatterplot of the middle eigenvalues of the n-vertex molecular graph (For an n-electron π system, with eigenvalues are arranged in non-increasing order, for even n the HOMO eigenvalue is equal to that at position $n/2$ and the LUMO eigenvalue to that at position $n/2+1$, and for odd n the HOMO and LUMO eigenvalues are necessarily equal to each other and to the eigenvalue at position $(n+1)/2$.) Chemically different types of electron configuration appear in distinct regions, and graphs with equal values of invariants appear along special lines: *isohomal*, *isolumal* and *isodiastemal* lines are the loci of graphs that share HOMO eigenvalues, LUMO eigenvalues and HOMO-LUMO gaps, respectively. A plausible conjecture for chemical graphs (simple, connected and of maximum degree ≤ 3) is that all but a finite number of exceptions lie within the 'chemical triangle ' of the map, with vertices at (HOMO, LUMO) $= (-1,-1)$, $(+1,-1)$ and $(+1,+1)$. It is proved that all chemical trees lie

within the triangle, as do all chemical graphs with up to 12 vertices. The smallest exceptional chemical graph is the Heawood graph, at $(+\sqrt{2}, -\sqrt{2})$

1 Introduction

This contribution introduces a simple diagrammatic representation of electron configurations of π-conjugated systems in terms of graph eigenvalues. The molecular graphs of fully conjugated π systems are the *chemical graphs*, i.e., those graphs that are simple, unweighted, connected, with maximum degree less than or equal to three.

In the simple Hückel model, there is a direct correspondence between adjacency eigenvalues λ_i, and eigenvectors $\mathbf{x}_i$, of the molecular graph and the orbital energies and molecular orbitals of the π system.[1] Graphs treated here have n vertices and m edges. If $\{\lambda_i\}$, $i = 1, \ldots, n$ are the eigenvalues of the molecular graph G_n arranged in non-increasing order,

$$\lambda_1 > \lambda_2 \geq \ldots \geq \lambda_n, \tag{1}$$

the orbital energies (from bonding ($\lambda > 0$) to antibonding ($\lambda < 0$)) are $\epsilon_i = \alpha + \lambda_i \beta$, where the coulomb integral α and resonance integral β, both negative energies, act as origin and unit of the energy scale. Multiple eigenvectors with a common eigenvalue correspond to degenerate orbitals and can be assumed to be an orthonormal set.

Motivated by the notion of the electronic configuration of a molecule, we can define an 'electronic configuration of a graph' as a vector of occupation numbers $\mathbf{e} = (n_1, n_2, \ldots, n_n)$ such that $0 \leq n_i \leq 2$ and the entries n_i sum to the number of electrons. An eigenvector $\mathbf{x}_i$ is 'unoccupied' or 'empty' if $n_i = 0$, 'partly occupied' if $n_i = 1$ and 'occupied' or 'full' if $n_i = 2$.

Given the set of energy levels, the ground-state electron configuration of the molecule and hence of the graph is determined by application of three rules: the Aufbau Principle (fill orbitals in order of decreasing eigenvalue), the Pauli Principle (no orbital may contain more than two electrons), and Hund's Rule of Maximum Multiplicity (no orbital receives second electron before all orbitals degenerate with it have each received one).[2] A molecule and its graph are *open shell* if any orbitals/eigenvectors are partially occupied, *closed shell* otherwise. For the ground

state, the entries n_i are non-increasing.

For neutral molecules, the order of the molecular graph, n, is equal to the number of electrons in the π system. The (fully or partly) occupied orbital of highest energy (least eigenvalue) is the HOMO ('highest occupied molecular orbital'). The (partly or fully) occupied orbital of lowest energy (greatest eigenvalue) is the LUMO (lowest unoccupied molecular orbital).[3] If there are partially occupied orbitals, HOMO and LUMO coincide; a partially occupied orbital is also known as a SOMO (singly occupied molecular orbital). In terms of the occupation numbers, the HOMO is the last orbital with $n_i > 0$, and the LUMO is the first with $n_i < 2$. λ_{HOMO} is the eigenvalue of the HOMO and of all orbitals degenerate with it; likewise λ_{LUMO} is the eigenvalue of the LUMO and of all orbitals degenerate with it.

For even n, it is easily seen that $\lambda_{\mathrm{HOMO}} = \lambda_{n/2}$ and $\lambda_{\mathrm{LUMO}} = \lambda_{n/2+1}$, as we can imagine first filling orbitals with two electrons each, according to the Aufbau and Pauli Principles, which will lead to $e_{n/2} = 2$ and $e_{n/2+1} = 0$, then invoking Hund's Rule if the first procedure leaves a degeneracy between occupied and unoccupied orbitals. As the only effect of Hund's Rule is to redistribute occupancies within a set of degenerate orbitals, the HOMO and LUMO eigenvalues are unchanged in the second stage. A similar argument shows $\lambda_{\mathrm{HOMO}} = \lambda_{\mathrm{LUMO}} = \lambda_{(n+1)/2}$ for odd n.

Within the Hückel approximations, the total π energy of the molecule is the sum of the orbital energies, weighted by their occupation numbers, $E_\pi = \sum_k n_k \lambda_k$. A related quantity, not in general equal to E_π, is the *graph energy*,[6] $E_G = \sum_k |\lambda_k|$. E_π and E_G are equal for the ground states of bipartite graphs and some others. E_π is sometimes denoted E_H (H for Hückel).

2 Electronic configurations

One of the basic questions about a molecular system is the characterisation of its electronic configuration. Electron configurations fall into six natural classes based on the energies (eigenvalues) of the frontier orbitals.

(i) If all orbitals contain either zero or two electrons, the system is a *closed shell*. Clearly, all closed-shell systems have even n. Closed shells fall into three sub-classes:[4]

(ia) *Pseudo-closed*: $\lambda_{\mathrm{LUMO}} > 0$,

(ib) *Properly closed*: $\lambda_{\mathrm{HOMO}} > 0 \geq \lambda_{\mathrm{LUMO}}$,

(ic) *Meta-closed*: $\lambda_{\mathrm{HOMO}} \leq 0$.

(ii) If there is an eigenvalue for which at least one orbital contains exactly one electron, the configuration is an *open shell*. Clearly, all systems with odd n are open-shell. Open-shell cases are not usually subdivided further, but it may be sometimes be useful to split open-shell systems into sub-classes by analogy with the closed-shells:

(iia) *Pseudo-open*: $\lambda_{\mathrm{HOMO}} = \lambda_{\mathrm{LUMO}} > 0$,

(iib) *Properly open*: $\lambda_{\mathrm{HOMO}} = \lambda_{\mathrm{LUMO}} = 0$,

(iic) *Meta-open*: $\lambda_{\mathrm{HOMO}} = \lambda_{\mathrm{LUMO}} < 0$.

The classifications have direct physical significance, encapsulated in chemical rules of thumb. A *pseudo-closed* or *pseudo-open* system has unused bonded capacity and may be expected to gain electrons or rearrange to improve the bonding effect of its electrons. Conversely, a *meta-closed* or *meta-open* system has antibonding (or nonbonding) electrons and may be expected to lose electrons or rearrange. The *properly closed* system matches bonding capacity and electron count and is *prima facie* a candidate for a stable π system, as larger gaps $\mid \lambda_{\mathrm{HOMO}} - \lambda_{\mathrm{LUMO}} \mid$ indicate greater stability. A *properly open* shell is likely to show facile gain and loss of electrons, and exhibit radical reactivity.

HOMO and LUMO eigenvalues give estimates of ionisation potentials and electron affinities, respectively: given the form of total π energy as a sum, at the Hückel level, a positive HOMO eigenvalue implies that the neutral molecule is more stable than the cation; a negative LUMO eigenvalue implies that the neutral is more stable than the anion.

These qualitative statements arise from a simplified analysis, and other effects may intervene in specific cases. In particular, Hückel theory does not take account of

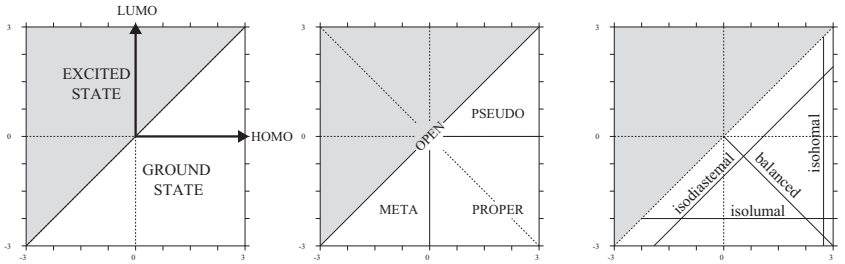

Figure 1: The HOMO-LUMO map (a) separates ground from excited states; (b) gives a geographical representation of the types of open and closed shell, and (c) groups those graphs that share an eigenvalue invariant along special straight lines.

electron repulsion, which causes the orbital energies to depend on occupation. However, within the graph theoretical approximation for electronic structure, eigenvalues give a clear first-order classification of the different types of electronic configuration.

3 The HOMO–LUMO map

The shell classification of electron configurations suggests a simple device for exhibiting characteristics of chemical graphs: a scatterplot of HOMO *vs* LUMO eigenvalues. It has the merit that qualitative distinctions between the different types of π shells emerge naturally as 'geographical' separations. Figure 1 shows the skeleton for such a plot.

The horizontal (HOMO) and vertical (LUMO) axes run from -ve (antibonding) to +ve (bonding). The 45° line $\lambda_{\mathrm{HOMO}} = \lambda_{\mathrm{LUMO}}$ represents the locus of open shells, and separates ground- and excited-state configurations: all ground states must have $\lambda_{\mathrm{HOMO}} \geq \lambda_{\mathrm{LUMO}}$ by Aufbau (Figure 1(a)). The region below the open-shell line defines the three kinds of closed shell: the bottom right quadrant defines the properly closed shells; the triangular region to the left defines the meta-closed shells, and the triangular region to the top right defines the pseudo-closed shells (Figure 1(b)). Other lines also have specific chemical meanings (Figure 1(c)). The line with slope +1 through the point $(\lambda_{\mathrm{HOMO}}, \lambda_{\mathrm{LUMO}})$ is occupied by graphs with

equal gap $\lambda_{\mathrm{HOMO}} - \lambda_{\mathrm{LUMO}}$. Adapting a term from dentistry, such graphs may be called *isodiastemal*.[1] A vertical line in the map represents graphs with equal λ_{HOMO} (*isohomal*); a horizontal line represents graphs with equal λ_{LUMO} (*isolumal*). The line $\lambda_{\mathrm{HOMO}} = -\lambda_{\mathrm{LUMO}}$ represents *balanced* graphs, where the bonding effect of the HOMO and the antibonding effect of the LUMO are equal; by the Pairing Theorem[8] all *bipartite* graphs are balanced in this sense. It is tempting to call the balanced but non-bipartite graphs *pseudo-bipartite*.

A special region of the HOMO-LUMO map, which for reasons that will emerge we call the *chemical triangle* is the right triangle with vertices $(-1, -1)$, $(+1, -1)$, $(-1, -1)$ with isolumal base, isohomal perpendicular and open-shell hypotenuse.

4 Bounds on HOMO and LUMO eigenvalues

Chemical graphs have maximum degree ≤ 3, and so the ranges of the axes in the plot are limited to

$$+3 \geq \lambda_{\mathrm{HOMO}} \geq \lambda_{\mathrm{LUMO}} \geq -3. \tag{2}$$

Calculations on thousands of graphs (see below) support the claim that most chemical graphs fit in the chemical triangle of the HOMO-LUMO map. In other words, we say that a chemical graph is *normal* if the following inequality holds:

$$+1 \geq \lambda_{\mathrm{HOMO}} \geq \lambda_{\mathrm{LUMO}} \geq -1. \tag{3}$$

Other chemical graphs are called *exceptional*.

By analogy with the spectral radius, we can define the *HOMO-LUMO radius* of a graph as $R = \max\{|\lambda_{\mathrm{HOMO}}|, |\lambda_{\mathrm{LUMO}}|\}$. A chemical graph G is normal if and only if $R(G) \leq 1$.

Chemically, the fact that for normal chemical graphs the inequality (3) holds

[1] A related phenomenon is termed *pseudo-isospectrality* by Jiang *et al.*:[7] this is the occurrence of graphs that have the same HOMO-LUMO gap, the same total π energy and the same even-order spectral moments. A pair of 16-vertex cubic polyhedral graphs with this combination of properties is noted in Ref. 7; for this pair, the frontier eigenvalues are not pairwise equal; λ_{HOMO} of one graph is $-\lambda_{\mathrm{LUMO}}$ of the other, so the two members of the pair occupy distinct points on the isodiastemal line.

corresponds to a claim that HOMO and LUMO orbital energies of every π system fall between the bonding and antibonding energies of the fixed double bond of ethene, represented by the chemical graph K_2, with eigenvalues ± 1. The implied ± 1 bounds are all realised multiple times, with the corners of the triangular region occupied by, e.g., K_3, K_4, ... at $(-1,-1)$, K_2, C_6, the cube, ... at $(+1,-1)$, a 9-vertex subdivision of $K_{3,3}$, the Petersen graph, ... at $(+1,+1)$.

Interestingly, both (the presumed vast majority of) chemical graphs (with low maximum degree) and the complete graph K_n (with degree $n-1$ and $\lambda_{\mathrm{HOMO}} = \lambda_{\mathrm{LUMO}} = -1$ for all $n \geq 2$) fall in the central region of the map. This observation might perhaps be taken to indicate that all simple, connected, unweighted graphs fall in this restricted region of the HOMO-LUMO map, but such an extension would certainly be incorrect. Computer search (see below) shows that, once the condition on maximum degree is relaxed, (non-chemical) graphs with $\lambda_{\mathrm{LUMO}} < -1$ appear at $n = 6$, and with $\lambda_{\mathrm{HOMO}} < -1$ (and $\lambda_{\mathrm{LUMO}} < -1$) appear at $n = 9$.

In fact, despite the weight of the numerical evidence (that, e.g., all chemical graphs on 13 or fewer vertices, and the many millions of fullerene graphs tested here, are normal), there do exist exceptional chemical graphs, with the smallest (and so far only) example being the 14-vertex, bipartite, 3-regular Heawood graph,[9] which has $\lambda_{\mathrm{HOMO}} = -\lambda_{\mathrm{LUMO}} = \sqrt{2}$. Chemically, this graph corresponds to the smallest (highly strained) 'polyhedral' polyhex nanotorus.[10]

However, exceptional chemical graphs seem to be quite difficult to find. For example, there are no further instances amongst the chemical graphs on 14 to 18 vertices, no more amongst the 3-regular graphs on 20 or fewer vertices, and no more amongst toroidal polyhex graphs on 100 or fewer vertices. We risk the following conjecture:

Conjecture 4.1 *There are only finitely many exceptional chemical graphs.*

The commonality between chemical and complete graphs raises an intriguing analogy with another graph invariant, the so-called graph energy.[6] The complete graph K_n has $E_G(K_n) = 2(n-1)$ and this is an upper bound for the graph energy of chemical graphs on n vertices.[11] However, it is *not* a bound for general graphs. If

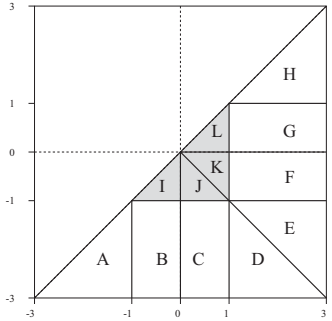

Figure 2: Nomenclature for the regions of ground-state space in the HOMO-LUMO map. Regions A to E are hypolumal (A being also hypohomal), D to H hyperhomal (H being also hyperlumal), and I to L lie in the chemical triangle (shaded), with I being meta-closed, J and K properly closed and L pseudo closed.

graphs G_n with $E_G(G_n) > E_G(K_n)$ are *hyperenergetic*,[12,13] we can define *hyperhomal* and *hypohomal* graphs as those for which $\lambda_{\mathrm{HOMO}}(G_n) > +1$ and $\lambda_{\mathrm{HOMO}}(G_n) > -1$, respectively. Likewise, *hyperlumal* and *hypolumal* graphs have $\lambda_{\mathrm{LUMO}}(G_n) < -1$ or $\lambda_{\mathrm{LUMO}}(G_n) > +1$, respectively. See Figure 2 for the demarcation lines of these regions.

Although not all chemical graphs are normal, two special families are of interest.

Theorem 4.2 *Each chemical tree (a tree with maximal degree at most* 3*) is normal.*

Proof. For a bipartite graph, $\lambda_{\mathrm{HOMO}} = -\lambda_{\mathrm{LUMO}} \geq 0$ and the HOMO-LUMO gap is $2\lambda_{\mathrm{HOMO}}$. If the graph is singular, $\lambda_{\mathrm{HOMO}} = \lambda_{\mathrm{LUMO}} = 0$ and the eigenvalue condition in the theorem is satisfied, so we need consider only non-singular chemical trees (and hence even values of n). Amongst the non-singular chemical trees (acyclic chemical graphs with perfect matchings), the *comb* has the largest gap.[14,15] The comb on $n = 2p$ vertices is constructed by attaching a leaf to each vertex of the path on p vertices and has eigenvalues[16]

$$\lambda_k^{\pm} = \frac{1}{2}\{\mu_k \pm \sqrt{\mu_k^2 + 4}\} \quad \text{for} \quad k = 1 \ldots p \tag{4}$$

where μ_k is an eigenvalue of the backbone path:

$$\mu_k = 2\cos(\pi p/p+1). \tag{5}$$

The HOMO eigenvalue of the comb is therefore

$$\lambda_p^+ = \cos(\pi p/p+1) + \sqrt{1+\cos^2(\pi p/p+1)}, \tag{6}$$

decreasing monotonically from 1 to $\sqrt{2}-1$ as p runs from 1 to ∞. It follows that $+1 \geq \lambda_{\rm HOMO} \geq 0 \geq \lambda_{\rm LUMO} \geq -1$ holds for all combs, and hence for all chemical trees. □

An eigenvalue bound for all bipartite and pseudo-bipartite chemical graphs follows from consideration of the graph energy. For a bipartite or pseudo-bipartite graph G, the HOMO and LUMO eigenvalues are those with the smallest magnitude, and the graph energy satisfies

$$E_G(G) \geq n|\lambda_{\rm HOMO}| \quad \text{for bipartite pseudo}-\text{bipartite graphs.} \tag{7}$$

As no chemical graph has an energy E_G greater than that of the complete graph,[11] the bounds

$$(2n-2) \geq E_G(G) \geq n|\lambda_{\rm HOMO}| \tag{8}$$

hold for all bipartite and pseudo-bipartite chemical graphs G, and the eigenvalue bound $+2 \geq \lambda_{\rm HOMO} \geq 0 \geq \lambda_{\rm LUMO} \geq -2$ applies to such graphs. A better upper bound on graph energy[17] improves the eigenvalue bounds:

Theorem 4.3 *If G is a bipartite or pseudo-bipartite graph with average degree $\bar{d} = 2m/n$, its* HOMO *and* LUMO *eigenvalues satisfy $\sqrt{\bar{d}} \geq \lambda_{\rm HOMO} \geq 0 \geq \lambda_{\rm LUMO} \geq -\sqrt{\bar{d}}$.*

Remark 4.4 For chemical graphs, $\bar{d} \leq 3$ and hence for bipartite and pseudo-bipartite chemical graphs $\sqrt{3} \geq \lambda_{\rm HOMO} \geq 0 \geq \lambda_{\rm LUMO} \geq -\sqrt{3}$.

Proof. The McClelland bound for graph energy[17] is $E_G \leq \sqrt{2mn}$, with equality

realised only for graphs with all eigenvalues of equal magnitude.[18] The definition of average degree and the bound (7) give $n\sqrt{\bar{d}} = \sqrt{2mn} \geq n\lambda_{\rm HOMO}$ for both bipartite and pseudo-bipartite graphs. □

Remark 4.5 For graphs G with properly closed shells, $\lambda_{\rm HOMO} > 0 \geq \lambda_{\rm LUMO}$ and $E_G(G) \geq \frac{n}{2}\{|\lambda_{\rm HOMO}| + |\lambda_{\rm LUMO}|\} = \frac{n}{2}\{\lambda_{\rm HOMO} - \lambda_{\rm LUMO}\}$. Therefore, the HOMO-LUMO gap is $\leq 2\sqrt{\bar{d}}$ and the smaller of $\lambda_{\rm HOMO}$ and $|\lambda_{\rm LUMO}|$ is $\leq \sqrt{\bar{d}}$.

Remark 4.6 The bounds of Theorem 4.2 can be improved for unicyclic bipartite chemical graphs. It is conjectured[18] that for $n \leq 7$ and $n = 9, 10, 11, 13$ and $n = 15$ the unicyclic chemical graph of maximum energy is a cycle, and at all other values of n it is the graph P_n^6 consisting of a hexagonal cycle with a path attached to one vertex. It has been proved that of all unicyclic graphs of order n that are not cycles, the graphs P_n^6 maximise the graph energy.[19]

Exhaustive calculations for chemical graphs with $n \leq 12$ show that the bounds in inequality (3) are satisfied. Numerical calculations on the graphs P_n^6 indicate that $E_G(G)/n$ is a monotonically decreasing function of n for this family of graphs, and hence that

$$+q \geq \lambda_{\rm HOMO} \geq 0 \geq \lambda_{\rm LUMO} \geq -q \tag{9}$$

where $q \approx 1.28525299$ is $E_G(P_{14}^6)/n$.

Remark 4.7 Better (n, m) bounds for E_G are available. For bipartite graphs[20]

$$E_G \leq 2(2m/n) + \sqrt{(n-2)(2m - 2(2m/n)^2}. \tag{10}$$

This expression approaches $n\bar{d}$ from below as n goes to infinity, and in the limit does not improve the eigenvalue bound derived from McClelland's theorem.

5 HOMO–LUMO profiles of some classes of chemical graphs

General chemical graphs were generated with McKay's program *geng*.[21] Spectra were calculated by Jacobi numerical diagonalisation, with an estimated absolute

accuracy of better than 10^{-12}, but for plotting purposes the data points are collected in bins of width 0.001. Chemical graphs may be classified by electron configuration, according to the 6 subclasses of open and closed shells, as defined earlier.

They may also be partitioned into five disjoint (δ, δ) classes according to minimum (δ) and maximum (Δ) degree (Table 1). Table 2 shows both types of breakdown for chemical graphs with at most 12 vertices. The counts are seen to be dominated by properly-closed shells for even n and properly-open shells for odd n.

Class	Δ	δ	
a	2	1	paths
b	2	2	cycles
c	3	1	
d	3	2	
e	3	3	3-regular

Table 1: Chemical graphs classified by minimum (δ) and maximum (Δ) degrees.

Figure 3 shows the HOMO-LUMO maps for the 306 chemical graphs on $n \leq 8$ vertices, the 2750 chemical graphs on $n \leq 10$ vertices, and the 27524 chemical graphs on $n \leq 12$ vertices. The immediate visual impression is of growing clustering in the properly-closed quadrant, but with significant proportions of pseudo- and meta-closed shells. The numerical data in Table 1 show that in the sample of graphs

n	N	(δ, Δ) classes			Open				Closed			
		(c)	(d)	(e)	N_O	ps	pr	me	N_C	ps	pr	me
2	1	0	0	0	0	0	0	0	1	0	1	0
3	2	0	0	0	2	0	1	1	0	0	0	0
4	6	2	1	1	3	0	2	1	3	0	2	1
5	10	5	3	0	10	1	7	2	0	0	0	0
6	29	17	8	2	9	0	9	0	20	0	15	5
7	64	42	20	0	64	7	41	16	0	0	0	0
8	194	133	54	5	52	1	50	1	142	2	103	36
9	531	382	147	0	531	57	321	153	0	0	0	0
10	1733	1274	438	19	453	2	448	3	1280	11	896	373
11	5524	4170	1352	0	5524	622	3330	1572	0	0	0	0
12	19430	14863	4480	85	4851	1	4842	8	14579	155	10170	4254

Table 2: Types of chemical graphs sorted by minimum and maximum degree. N is the number of chemical graphs on n vertices. Types (a) to (e) are defined in Table 1 At each $n > 2$, the degree classes (a) and (b) each contain one graph. N_O and N_C are the numbers of open and closed shells at each n, respectively, partitioned into pseudo (ps), proper (pr) and meta (me) sub-classes.

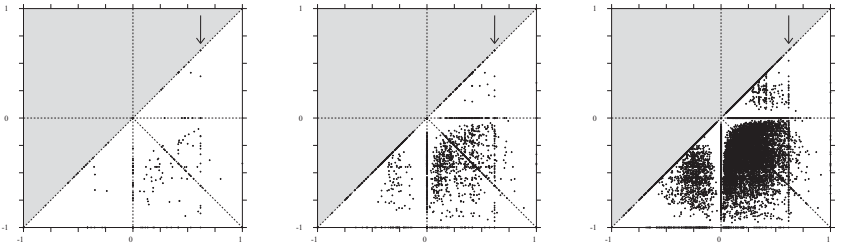

Figure 3: The HOMO-LUMO map of all chemical graphs with (from left to right) up to 8, up to 10, and up to 12 vertices. In this figure, eigenvalues are sorted into bins of width 0.001, each represented on the plot by a circle of diameter 0.005. The arrow indicates the golden isohomal line at $\lambda_{\mathrm{HOMO}} = \phi^{-1}$.

with $n \leq 12$ there are 11187 properly closed, 168 pseudo-closed, 4670 meta-closed (of which 1237 have an antibonding HOMO), and 11499 open shells. Many (6131) open shells come from the odd-n graphs. Of the open shells, 9051 have $\lambda_{\mathrm{HOMO}} = \lambda_{\mathrm{LUMO}} = 0$.

Inspection of the pattern also reveals line clustering: a scatter of graphs on the boundary lines $\lambda_{\mathrm{HOMO}} = +1$ and $\lambda_{\mathrm{LUMO}} = -1$, a line of graphs with $\lambda_{\mathrm{HOMO}} = (\sqrt{5}-1)/2 = \phi^{-1} \approx 0.618$, as well as heavily populated lines for $\lambda_{\mathrm{HOMO}} = \lambda_{\mathrm{LUMO}}$ and $\lambda_{\mathrm{HOMO}} = -\lambda_{\mathrm{LUMO}}$. Eigenvalues $\pm\phi$ and $\pm\phi^{-1}$ are often found for chemical

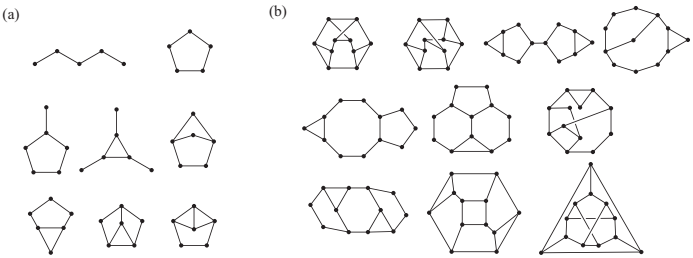

Figure 4: Some special chemical graphs: (a) the smallest that have HOMO eigenvalue ϕ^{-1}; (b) the smallest pseudo-bipartite chemical graphs. Graphs drawn with edge crossings are non-planar.

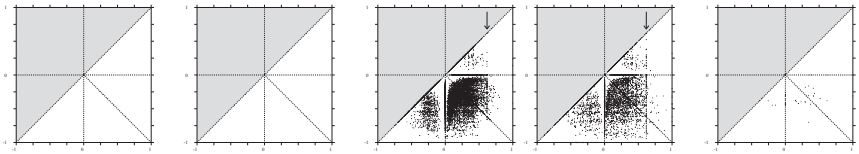

Figure 5: Cumulative HOMO-LUMO maps for the types (a) to (e) of chemical graphs (as defined in Table 1) on $n \leq 12$ vertices. The arrow indicates the golden isohomal line at $\lambda_{\mathrm{HOMO}} = \phi^{-1}$.

graphs, and just over 1% of the chemical graphs on $n \leq 12$ vertices have $\lambda_{\mathrm{HOMO}} = \phi^{-1}$. The 'golden' isohomal line, with $\lambda_{\mathrm{HOMO}} = \phi^{-1}$, is clearly visible in Fig. 3 (and later in Fig. 5(c)(d), not only because it is heavily populated, but because it represents a dividing line, with greater density of dots to the left. It is not clear why one eigenvalue should stand out in this way. Some small chemical graphs with this HOMO eigenvalue are illustrated in Figure 4(a). Some small chemical graphs that are balanced but not bipartite are illustrated in Figure 4(b).

Figure 5 gives an impression of how the different (δ, Δ) degree classes contribute to the composite HOMO-LUMO map for the chemical graphs on $n \leq 12$ vertices. Clearly, the maps for the two largest classes are strikingly similar to the composite map. The 3-regular graphs on up to 12 vertices include no examples of pseudo-closed shells, but these appear at higher vertex count.

Paths (the molecular graphs of linear polyenes) are of course bipartite. Paths P_n with odd numbers of vertices n all inhabit the origin in the HOMO-LUMO plot, with $\lambda_{\mathrm{HOMO}} = \lambda_{\mathrm{LUMO}} = 0$. The path P_n with an even number of vertices n has $\lambda_{\mathrm{HOMO}} = -\lambda_{\mathrm{LUMO}} = 2\cos[\pi n/2(n+1)]$; with increasing n, the configuration moves in along the line of balanced properly closed shells, from $(+1, -1)$ for P_2, though $(+0.618, -0.618)$, $(+0.445, -0.445)$, $(+0.347, -0.347)$, ..., to converge on the origin (See Figure 5(a)).

Cycles (the molecular graphs of $[n]$ annulenes) have either open or properly closed shells as neutral systems. The two classes of bipartite cycles are: even cycles C_n with $n = 4p$, with two zero eigenvalues and hence properly open shells with $\lambda_{\mathrm{HOMO}} =$

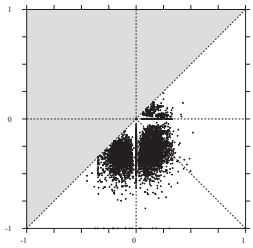

Figure 6: HOMO-LUMO map for the 7595 20-vertex cubic polyhedra.

$\lambda_{\rm LUMO} = 0$; even cycles C_n with $n = 4p + 2$, which have no zero eigenvalue and so have properly closed shells with $\lambda_{\rm HOMO} = -\lambda_{\rm LUMO} = 2\cos[2\pi p/(4p + 2)]$. Odd cycles all have properly open shells as neutrals: those with $n = 4p+1$ have $\lambda_{\rm HOMO} = \lambda_{\rm LUMO} = 2\cos[2\pi p/(4p + 1)]$, and those with $n = 4p + 3$ have $\lambda_{\rm HOMO} = \lambda_{\rm LUMO} = 2\cos[2\pi(p + 1)/(4p + 3)]$. On the HOMO-LUMO map, the 'anti-aromatic' $n = 4p$ cycles all lie at the origin, the 'aromatic' cycles with $n = 4p+2$ approach the origin along the 45° line from bottom right, and the odd cycles with $n = 4p + 1$ and $n = 4p + 3$ approach the origin along the open-shell line from $(+, +)$ and $(-, -)$ quadrants, respectively (See Figure 5(b)).

Cubic Polyhedra. These are candidates for the structures of the smaller carbon clusters C_n and also include the underlying skeletons of polyhedral $(CH)_n$ hydrocarbons. Their graphs were generated using the *plantri* program.[25] The numbers of cubic polyhedral graphs $N_P(n)$ at each vertex count n are: 1 (4), 1 (6), 2 (8), 5 (10), 14 (12), 50 (14), 233 (16), 1249 (18), 7595 (20), 49566 (22), ... As an example, Figure 6 shows the map for the 7595 20-vertex cubic polyhedra. Given the large number of polyhedra with triangular ('electron-deficient') faces, it is not surprising that the meta-closed region of the map is heavily populated, as is the properly closed quadrant. The numerical data show 2245 meta-closed, 4291 properly closed, 245 pseudo-closed and 76 open shells in this sample. Dodecahedral C_{20}, the smallest possible fullerene, is only one of 70 graphs at $(0, 0)$.

Fullerenes have molecular graphs that are cubic and polyhedral with 12 pentagonal

and $(n/2 - 10)$ hexagonal faces. A small subset, including icosahedral C_{60},[22] have *properly closed* shells, but the overwhelming majority of fullerenes have *pseudo-closed* character,[23] with a few large fullerene graphs known to have *meta-open* character.[24] The maps in Figure 7 illustrate this in dramatic fashion: of the 1812 fullerene isomers with 60 vertices, all but one are found in the pseudo-closed region of the map (Figure 7(a)); likewise, of the 8149 fullerene isomers of C_{70}, only the unique isolated-pentagon isomer is properly closed, lying on the $\lambda_{\mathrm{HOMO}} = 0$, boundary line between pseudo- and properly closed classes (Figure 7(b)). Most isolated-pentagon fullerenes are also pseudo-closed, as illustrated by the set of the 10774 IPR fullerenes with $n = 120$ (Figure 7(c)); just 42 of these have properly closed shells, of which 40 arise as a consequence of the leapfrog rule and the existence of a total of 40 isomers of the lower fullerene C_{40}, one more (with $\lambda_{\mathrm{LUMO}} = 0$) as an instance of the 'carbon cylinder rule', and one as an instance of a 'sporadic' closed shell.[23] This last isomer has a tiny LUMO eigenvalue of -0.0004, and so escapes pseudo-closed status by a very narrow margin, as of course does the carbon cylinder isomer ($\lambda_{\mathrm{LUMO}} = 0$). In Ref. 5, HOMO-LUMO maps of fullerenes are studied in more detail.

Beyond chemical graphs. Extending the *geng* generation process to all connected graphs, it was possible to find many examples outside the chemical triangle. The

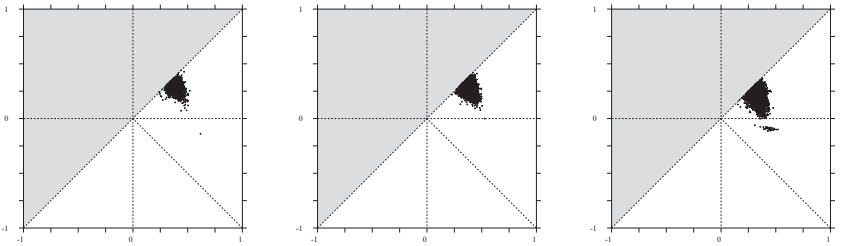

Figure 7: Fullerene HOMO-LUMO maps (a) The 1812 fullerene isomers of C_{60}. The single point in the closed-shell quadrant corresponds to the experimental icosahedral isomer of C_{60}. (b) The 8149 70-vertex fullerene isomers of C_{70}. The point on the line $\lambda_{\mathrm{HOMO}} = 0$ corresponds to the experimental isomer of C_{70}. (c) The 10774 isolated-pentagon fullerene isomers of C_{120}.

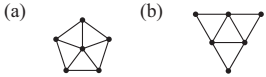

Figure 8: Graphs that fall outside the 'chemical triangle'. The two smallest graphs are of order $n = 6$, with (a) $m = 10$, $\lambda_{\rm HOMO} = \phi^{-1}$, $\lambda_{\rm LUMO} = 1 - \sqrt{6} \approx -1.4495$, (b) $m = 9$, $\lambda_{\rm HOMO} = \phi^{-1}$, $\lambda_{\rm LUMO} = 1 - \sqrt{5} \approx -1.2361$.

connected graphs $N_G(n)$ at each vertex count n are:[26] 1 (2), 2 (3), 6 (4), 21 (5), 112 (6), 853 (7), 11117 (8),261080 (9), 11716571 (10), 1006700565 (11), 164059830476 (12), 50335907869219(13) ... All connected graphs with $n \leq 5$ or $n = 7$ fall in the chemical triangle map. *Hyperlumal* graphs appear first at $n = 6$, where there are two examples (Figure 8). There are 119 with $n = 8$, and 12 to 22 edges. At $n = 9$, 37 graphs with 18 to 26 edges are both hypohomal and hyperlumal. At $n = 10$, 151062 graphs occur outside the chemical region of the HOMO-LUMO map: 151055 are hyperlumal only but 7 are both hypohomal and hyperlumal, all seven having $\lambda_{\rm HOMO} < -1$ and $\lambda_{\rm LUMO} = -\sqrt{2}$.

6 Acknowledgements

TP was supported by ARRS Grant PI-0294. PWF thanks the Royal Society for an award under the RS/Wolfson Research Merit Scheme, and his dentist, Mr Barry N. Hunt (LDS), for filling a notational gap. We thank Gaspar Jaklič for pointing out the Heawood graph ahead of the computer, and Gunnar Brinkmann for computing polyhex adjacency data.

References

[1] I. Gutman, O. E. Polansky, *Mathematical Concepts in Organic Chemistry*, Springer–Verlag, Berlin, 1986.

[2] C. E. Housecroft, A. G. Sharpe, *Inorganic Chemistry*, Pearson Education, Harlow, 2008.

[3] IUPAC. *Compendium of Chemical Terminology, 2nd ed. (The 'Gold Book')*. Compiled by A. D. McNaught, A. Wilkinson, Blackwell Scientific Publications, Oxford, 1997.

[4] P. W. Fowler, T. Pisanski, Leapfrog fullerenes and Clar polyhedra, *J. Chem. Soc. Faraday Trans.* **90** (1994) 2865–2871.

[5] P. W. Fowler, T. Pisanski, HOMO-LUMO maps for fullerenes, *Acta Chem. Slov.*, submitted.

[6] I. Gutman, The energy of a graph, *Berichte der Mathematisch–Statistischen Sektion im Forschungszentrum Graz* **103** (1978) 1–22.

[7] Y. S. Jiang, Y. H. Shao, E. C. Kirby, Topology and stability of trivalent polyhedral clusters, *Fullerene Sci. Techn.* **2** (1994) 481–487.

[8] C. A. Coulson, G. S. Rushbrooke, Note on the method of molecular orbitals, *Proc. Camb. Phil. Soc.* **36** (1940) 193–200.

[9] D. Cvetković, M. Doob, H. Sachs, *Spectra of Graphs – Theory and Application*, Academic Press, New York, 1980; 2nd revised ed.: Barth, Heidelberg, 1995.

[10] E. C. Kirby, R. B. Mallion, P. Pollak, Toroidal polyhexes, *J. Chem. Sci. Faraday Trans.* **89** (1993) 1945–1953.

[11] I. Gutman, Y. Hou, H. B. Walikar, H. S. Ramane, P. R. Hampiholi, No Hückel graph is hyperenergetic, *J. Serb. Chem. Soc.* **65** (2000) 799–801.

[12] I. Gutman, Hyperenergetic molecular graphs, *J. Serb. Chem. Soc.* **64** (1999) 199–205.

[13] J. H. Koolen, V. Moulton, I. Gutman, D. Vidović, More hyperenergetic molecular graphs, *J. Serb. Chem. Soc.* **65** (2000) 571–575.

[14] J. Y. Shao, Y. Hong, Bounds on the smallest positive eigenvalue of a tree with perfect matchings, *Chin. Sci. Bull.* **37** (1992) 713–717.

[15] F. Zhang, C. An, Acyclic molecules with greatest HOMO–LUMO separation, *Discr. Appl. Math.* **98** (1999) 165–171.

[16] P. W. Fowler, P. Hansen, G. Caporossi, A. Soncini, Polyenes with maximum HOMO–LUMO gap, *Chem. Phys. Lett.* **342** (2001) 105–112.

[17] B. J. McClelland, Properties of the latent roots of a matrix: the estimation of π-electron energies, *J. Chem. Phys.* **54** (1971) 640–643.

[18] G. Caporossi, D. Cvetković, I. Gutman, P. Hansen, Variable Neighbourhood Search for extremal graphs. 2. Finding graphs with extremal energy, *J. Chem. Inf. Comput. Sci.* **39** (1999) 984–996.

[19] Y. Hou, I. Gutman, C. W. Woo, Unicyclic graphs with maximal energy, *Lin. Algebra Appl.* **356** (2002) 27–36.

[20] J. H. Koolen, V. Moulton, Maximal energy bipartite graphs, *Graphs and Combinatorics* **19** (2003) 131–135.

[21] B. D. McKay, *Geng* is part of the *gtools* utilities associated with the graph isomorphism-automorphism software nauty, the manual for which is available at http://cs.anu.edu.au/∼bdm/nauty.

[22] H. W. Kroto, J. R. Heath, S. C. O'Brien, R. F. Curl, R. E. Smalley, C_{60}: Buckminsterfullerene, *Nature* **318** (1985) 162–163.

[23] P. W. Fowler, D. E. Manolopoulos, *An Atlas of Fullerenes*, Oxford Univ. Press, 1995, Dover Publications, 2006.

[24] P. W. Fowler, Fullerene graphs with more negative than positive eigenvalues: The exceptions that prove the rule of electron deficiency? *J. Chem. Soc. Faraday Trans.* **93** (1997) 1–3.

[25] G. Brinkmann, B. D. McKay, Fast generation of planar graphs, *MATCH Commun. Math. Comput. Chem.* **58** (2007) 323–357

[26] Sequence A001349 *in* N. J. A. Sloane, *The On–Line Encyclopedia of Integer Sequences*, published electronically at www.research.att.com/∼njas/sequences/ , 2008.